

Accepted Manuscript

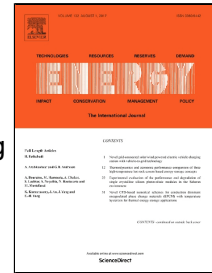
Energy, exergy and environmental analysis of a novel combined system producing power, water and Hydrogen

Kiyan Parham, Hamed Alimoradiyan, Mohsen Assadi

PII: S0360-5442(17)31008-3
DOI: 10.1016/j.energy.2017.06.016
Reference: EGY 11020
To appear in: *Energy*
Received Date: 30 January 2017
Revised Date: 16 May 2017
Accepted Date: 04 June 2017

Please cite this article as: Kiyan Parham, Hamed Alimoradiyan, Mohsen Assadi, Energy, exergy and environmental analysis of a novel combined system producing power, water and Hydrogen, *Energy* (2017), doi: 10.1016/j.energy.2017.06.016

This is a PDF file of an unedited manuscript that has been accepted for publication. As a service to our customers we are providing this early version of the manuscript. The manuscript will undergo copyediting, typesetting, and review of the resulting proof before it is published in its final form. Please note that during the production process errors may be discovered which could affect the content, and all legal disclaimers that apply to the journal pertain.



Energy, exergy and environmental analysis of a novel combined system producing power, water and Hydrogen

Kiyan Parham ^{1,*}, Hamed Alimoradiyan ², Mohsen Assadi ¹

¹ Department of Petroleum Engineering, Faculty of Science and Technology, University of Stavanger, 4036 Stavanger, Norway

² Department of Mechanical Engineering, Eastern Mediterranean University, G. Magosa, TRNC, Mersin 10, Turkey

* E-mail: kiyan.parham@uis.no

Fax: +47 51831750

Tel: +47 51833606

Abstract

During last years, absorption heat transformers have been used widely for boosting low-grade heat sources. In this paper, a novel multi-generation system including an open absorption heat transformer (OAHT), an organic Rankine cycle with Internal Heat Exchanger (ORC-IHE) and an electrolyzer for hydrogen production is proposed and analyzed from both first and second laws of thermodynamics and exergoenvironmental analysis points of view. To assess the cycle's performance, thermodynamic models were developed and a parametric study was carried out. The results indicate that the net power output and the hydrogen production rate will increase by boosting the inlet temperature of the waste heat using OAHT. By the growth of evaporator temperature, exergoenvironmental impact index, exergetic stability factor and exergetic sustainability index is increasing which is advantageous for the environment.

Keywords: Open absorption heat transformer, organic Rankine cycle with Internal Heat Exchanger, electrolyzer, energy, exergy, exergoenvironmental analysis.

Nomenclature

| | |
|------|--|
| AHT | absorption heat transformer |
| COP | coefficient of performance |
| CV | Control volume |
| DAHT | double stage absorption heat transformer |
| EES | Engineering Equation Solver |
| f | flow ratio |
| GTL | Gross temperature lift |
| h | enthalpy (kJ/kg) |
| IHE | internal heat exchanger |

| | | |
|----|------------|--|
| 39 | \dot{m} | mass flow rate (kg/s) |
| 40 | OAHT | Open absorption heat transfer |
| 41 | P | pressure |
| 42 | PR | performance ratio |
| 43 | Q | heat capacity (kW) |
| 44 | SAHT | single stage absorption heat transformer |
| 45 | SFEE | Steady-flow energy equation |
| 46 | S-ORC | Simple organic Rankine Cycle |
| 47 | THAT | triple stage absorption heat transformer |
| 48 | turb | turbine |
| 49 | X | concentration |
| 50 | ΔX | concentration difference |

51
52 **Subscript**

| | | |
|----|-----|------------------|
| 53 | 0 | ambient property |
| 54 | abs | absorber |
| 55 | con | condenser |
| 56 | eva | evaporator |
| 57 | gen | generator |
| 58 | s | strong |
| 59 | w | weak |

60

61 **I. Introduction**

62 During recent past, great interest has been focused on employing mid/low-level temperature heat sources
63 from industries, solar radiation and geothermal heat source [1]. In fact, these heat sources represent a
64 considerable amount of energy by the capability of being recycled in secondary heat recovery technologies
65 such as organic Rankine cycles (ORCs) [2] Kalina cycle [3], absorption refrigeration systems [4-6], and
66 heating implements [7]. The second type refrigeration cycles, also called absorption heat transformers
67 (AHTs), stand as the superlative relevant applicants of getting benefit of mid/low-level heat sources [8].
68 Operating as reversed absorption heat pumps (AHPs), AHTs have the capability of boosting the low-grade
69 heat to higher temperature levels and thereby improving their usefulness by a negligible input of electric
70 power [9].

71 The first category of AHTs, known as single stage absorption heat transformers (SAHT), capable of
72 recovering about half of the input waste heat can supply the demanded energy of the succeeding industrial
73 processes [10]. The quantities of absorption effects has a main role on the temperature level of out-coming
74 heat from AHTs [11]. For single, double and triple AHTs, COPs (coefficient of performances) and GTLs
75 (gross temperature lifts) of about (0.5, 0.35 and 0.2) and (50, 80 and 140 °C) are accessible [9, 11, 12].

76 Solutions of LiBr–H₂O and NH₃–H₂O are the most commonly utilized pairs in absorption cycles [13].
77 Neglecting the crystallization problem of LiBr–H₂O systems, they have better performance in comparison
78 to NH₃–H₂O solutions [14]. Waste heat from different industrial plants, standing in mid-low level temperature
79 range has the potential to be employed as an appropriate heat source for AHTs [15]. Higher temperatures
80 of waste heat to be utilized in auxiliary processes can be gained easily by these systems [8]. This
81 outstanding characteristic of AHT sorts them a worthy candidate to be used in desalination applications
82 [16]. Within last decade a huge attention has been paid to integrating absorption cycles into desalination
83 set-ups [12, 15]. For instance, open absorption heat transformer (OAHT) were coupled to single and
84 multiple desalination systems [17, 18] and demonstrated the aptitude of having higher COPs than those of
85 common AHTs. The higher COP, the higher quantity of distilled water [18, 19].

86 OAHTs can also be connected to organic Rankine cycles. Owing the outstanding characteristics such as
87 structure simplicity and satisfactory economic besides thermodynamic aspects, ORCs can be integrated
88 with OAHTs as the secondary cycle. The integrated system has the capability of generating power by
89 means of low-temperature heat input [20]. Recently, Zare [21] applied thermodynamic and economic
90 analyses of three different configurations of organic Rankine cycles. It was demonstrated that the ORC
91 utilizing Internal Heat Exchanger (ORC-IHE) had the best performance concerning the first and second
92 laws of thermodynamic. A similar trend has also been reported by Yari [20] through thermodynamic analysis
93 of different set ups of ORCs. Hydrogen production system can be a proper candidate as the subsequent
94 arrangement of ORC-IHE due to the organic Rankine cycle turbine power. Environmentally friendly
95 characteristics besides the feature of being a potential fuel for next generation vehicles dedicates Hydrogen
96 production a great importance. Conducted several studies have proved that the role of Hydrogen on
97 upcoming sustainable progress is going to be highlighted [22-24]. In the current research, a cogeneration
98 cycle comprising of an OAHT, an ORC-IHE and an electrolyzer for supplying power, distilled water, and
99 hydrogen is studied both from first and second laws of thermodynamics. For the aim of investigating the
100 effects of imperative variables such as waste water inlet temperature, turbine inlet temperatures and
101 pressure, gross temperature lift and generation temperature on the cycle performance and Hydrogen
102 production a code has been developed in Engineering Equation Solver (EES) [25] and a comprehensive
103 parametric study has been carried out. Additionally, an inclusive exergoenvironmental analyses has also

104 be done.

105 **II. System description**

106 The combined cycle demonstrated in Fig. 1 is made up of an open absorption heat transformer, an organic
107 Rankine cycle, and an electrolyzer. The consisting elements of a basic AHT are a condenser, a generator,
108 an absorber, an evaporator, an expansion valve, a pair of pumps and a solution heat exchanger. Mid-low
109 level temperature heat is transferred to the working pair (LiBr/H₂O) through generator and is rejected from
110 condenser and absorber. In the generator, a portion of the solution water is evaporated and set off to
111 condenser. This will lead to increased solution concentration. The outgoing strong solution of LiBr+H₂O
112 from generator passes through economizer and then absorbs the water vapor coming from the evaporator.
113 Since the absorption process is exothermic, the absorber temperature will rise. The boosted heat from
114 absorber has the potential to provide the demanded heat for desalination set up. Following the absorber
115 that partially evaporates water, separator vessel divides the obtained two phase flow into vapor and liquid
116 phases. The latent heat of the water vapor is employed for evaporating the liquid part which goes back to
117 the absorber. Now the outgoing fluid from evaporator has the capability to drive organic Rankine cycle
118 (point 12). The obtained weak solution of the absorber is heated by economizer and then enters generator.
119 The main advantage of OAHT in comparison to common AHTs is that the condensed water from the
120 condenser is extracted as distilled water instead of flowing to the evaporator (stream 23, Fig. 1).
121 Considering the fact that some contaminations and impurities are to be accumulated within the evaporator,
122 a portion of the outgoing flow from the evaporator (1/20 of the waste feed water of the system) is considered
123 as “discharged wastewater” denoted by stream 13. Next to open absorption heat transformer, ORC-IHE
124 utilizes the heat of absorber as the secondary cycle. A typical organic Rankine cycle (TORC) comprises a
125 pump, a condenser, an evaporator and a turbine. The evaporator has the role of heat source for ORC where
126 the passing working flow is heated. At the subsequent stage by fluid expansion through the turbine, power
127 is produced which is followed by a cooling process in the condenser and then flowing back to the evaporator
128 assisted by the pump.

129 It is worth mentioning that in contrary to common steam plants, the exiting fluid from the turbine for most of
130 the ORC fluids is in vapor phase rather than that of two-phase flow. By employing an Internal Heat
131 Exchanger (IHE) and recovering a portion of the available heat at the turbine outlet, the performance of the

132 ORC can be improved. The mid part of Fig. 1 demonstrates this set up which is denoted as organic Rankine
 133 cycle with Internal Heat Exchanger. As common power cycles, there's an additional aspect of this cycle
 134 stating that the properties of the working fluid have a great impact on its performance [21]. At the current
 135 study, Isobutane was selected as the working fluid considering the temperature of the heat source and the
 136 fluid properties. Half of the power produced by ORC-IHE is transferred to the electrolyzer where water is
 137 converted to hydrogen and oxygen. The produced hydrogen can be stored later use as per consumer need,
 138 and the oxygen can be used e.g. for performance improvement of digestion based biogas generator.

139

140 Fig. 1. Schematic illustration of the proposed cycle.

141

142 III. Thermodynamic model

143 A code is developed in Engineering Equation Solver (EES) for thermodynamic simulation of the latter
 144 mentioned proposed cycle. Any element of the system has been considered as a control volume and first
 145 and second laws of thermodynamic besides mass conservation principle have been employed on them.

146

147 III.1. First law analyses

148

149 The mass balance can be expressed as:

$$150 \quad \Sigma \dot{m}_{in} - \Sigma \dot{m}_{out} = 0 \quad (1)$$

151 Where \dot{m} stands for the fluid mass flow rate. Any element is treated as a steady state system as follows:

$$152 \quad \Sigma(\dot{m} h)_{in} - \Sigma(\dot{m} h)_{out} + \dot{Q}_{cv} - \dot{W}_{cv} = 0 \quad (2)$$

153 Here \dot{Q}_{cv} and \dot{W}_{cv} are the heat and power interactions of the CV with the surroundings.

154 Based on the thermal energy input to the integrated cycle, the thermal or first law efficiency may be
 155 expressed as follows:

$$156 \quad \eta_t = \frac{\dot{W}_{net}}{Q_{gen}} \quad (3)$$

157 where

$$158 \quad \dot{W}_{net} = \dot{W}_{turb} - \dot{W}_{pump} \quad (4)$$

159 The in depth mass and energy analysis which are very simple mathematical calculations are taken from
 160 those of Zhang et al. [17]. Due to not repeating them once more, they are not brought up here.

161 **III.2. Second law**

162 For evaluation of the systems' performance, use of the second law of thermodynamic has been emphasized
 163 due to its suitability for assessment of the selected system.

164 By neglecting kinetic, potential and chemical exergies the exergy of the fluid stream can be stated as:

$$165 \quad \dot{E} = \dot{m}[(h - h_o) - T_o(s - s_o)] \quad (5)$$

166 The exergy transferred by waste heat to the OAHT generator is assumed as input exergy and thus the
 167 second law efficiency of the proposed cycle is defined as:

$$168 \quad \eta_{II} = \frac{\dot{W}_{net}}{E_{in}} \quad (6)$$

169 For any element, the exergy destruction rate is calculated by the following equation:

$$170 \quad \dot{E}_{D,k} = \sum \dot{E}_{in,k} - \sum \dot{E}_{out,k} \quad (7)$$

171

172 **III.3. Performance evaluation**

173 In absorption cycles, COP is considered as the indicator of boosting the provided heat at given temperature
 174 of the evaporator and generator to the level of absorber temperature. For closed AHTs it is defined as
 175 follows:

$$176 \quad COP = \frac{\dot{Q}_{abs}}{\dot{Q}_{gen} + \dot{Q}_{eva}} \quad (8)$$

177 Where \dot{Q} stands for heat transfer rate (kW).

178 It is worth mentioning that in OAHTs, the demanded heat for evaporator (\dot{Q}_{eva}) is provided by absorber
 179 and hence no external heat source is needed which leads definition of the COP as:

180

$$181 \quad COP = \frac{\dot{Q}_{abs}}{\dot{Q}_{gen}} \quad (9)$$

182 One of the most imperative parameters in designing and optimizing absorption heat transformers, is the
 183 flowing ratio:

$$184 \quad f = \frac{\dot{m}_s}{\dot{m}_r} \quad (10)$$

185 in which \dot{m}_s and \dot{m}_r stand for strong solution and weak refrigerant mass flow rates (kg/s) respectively.

186 Similarly, in desalination systems, the quantity of distilled water over spent motive steam by generator is
187 called performance ratio (PR) and from the view point of design and optimization is of great importance:

$$188 \quad PR = \frac{\text{the amount of distilled water}}{\text{the amount of motive stream}} = \frac{D}{\dot{Q}_{gen}/r_{gen}} \quad (11)$$

189

190 (D and r_{gen} are the quantity of produced water and latent heat of water at generator temperature).

191 Gross temperature lift is the ability of AHT to increase the temperature of the available heat source to more
192 useful level. The temperature lift for OAHT is defined as [18]:

193

$$194 \quad \Delta T = T_{abs} - T_{gen} \quad (12)$$

195 **III. 4. Exergoenvironmental aspects**

196 Nowadays, environmental analysis is of great interest in different aspects of science. Studying combined
197 cycles only from the view point of energy and exergy does not seem to be satisfactory. Recently, exergy-
198 based environmental analyses and sustainability examines have been employed in Hydrogen production
199 cycles [24]. The effects of exergy efficiency and destruction on environmental subjects are the base of
200 exergoenvironmental analyses.

201 According to [26, 27] the chief exergoenvironmental parameters are as follows:

202 **A. Exergoenvironmental impact factor (f_{ei})**, which clarifies the optimistic impact of the system on
203 the environment for the aim of decreasing environmental harms through reduction of irreversibilities
204 which is defined as:

$$205 \quad f_{ei} = \frac{\dot{E}x_{des,tot}}{\sum \dot{E}x_{in}} \quad (13)$$

206 Where $\dot{E}x_{des,tot}$ and $\dot{E}x_{in}$ stand for total exergy destruction and provided exergy to the
207 system respectively.

208 **B. Exergoenvironmental impact index (θ_{ei})**, which determines if the system damages
 209 environment or not. The less exergoenvironmental impact index, the desired
 210 environmental performance.

$$211 \quad \theta_{ei} = f_{ei} * C_{ei} \quad (14)$$

212 While

$$213 \quad C_{ei} = \frac{1}{\frac{\eta_{ex}}{100}} \quad (15)$$

214 where C_{ei} and η_{ex} characterize exergoenvironmental impact coefficient and exergetic
 215 efficiency, correspondingly.

216 **C. Exergoenvironmental impact improvement (θ_{eii})**, which aims to discover the environmental
 217 relevance of the system. In contrary to the exergoenvironmental impact index, it would be as high
 218 as possible which revenues the fact that it is more beneficial to the environment.

$$219 \quad \theta_{eii} = \frac{1}{\theta_{ei}} \quad (16)$$

220 **D. Exergetic stability factor (f_{es})** is defined as:

$$221 \quad f_{es} = \frac{\dot{E}x_{tot,out}}{\dot{E}x_{tot,out} + \dot{E}x_{des,tot} + \dot{E}x_{uu}} \quad (17)$$

222 Where exergy $\dot{E}x_{uu}$ stands carried exergy by unused fuel (if any fuel is consumed in the system).
 223 Approaching to “one”, is the desired quantity for this parameter.

224 **E. Exergetic sustainability index (θ_{est})**, that is calculated as:

$$\theta_{est} = f_{es} * \theta_{eii} \quad (18)$$

It is evident that acquiring highest quantity of exergetic sustainability index is preferred.

III. 5. Validation of the results

The results of Rivera et al. [28] for a single stage absorption heat transformer, have been used for verifying the achieved outcomes of the current study. By assuming the same input data ($T_{gen} = T_{eva} = 74.1$ °C and $T_{con} = 20$ °C) and conditions in terms of negligible pressure and heat drops in pipes, isenthalpic expansion valve and 70% efficiency for economizer, our results correspond to those of their outcomes. Fig. 2 demonstrates the comparison of absorber temperature versus flow ratio by a negligible relative, which is completely reasonable.

Fig. 2. Comparison of the simulation results with those of Rivera et al [28].

Tables 1 and 2 demonstrate the input assumptions and operational properties for any point.

Table. 1. The Initial Design and Operation Parameters of the System.

Table. 2. Thermodynamic properties of the System at each state point.

IV. Results and discussion

The effect of T_{gen} on the COP of OAHT and the performance ratio have been plotted in Fig. 3. The COP decreases exponentially as T_{gen} increases. This is in contrast to the results obtained for a closed AHT in Ref. [8] wherein by increasing T_{gen} , COP enhanced. This is completely reasonable according to equation 9 which is basically different from definition of COP for common AHTs. In OAHT, \dot{Q}_{abs} correspondingly covers \dot{Q}_{eva} and so \dot{Q}_{eva} is not considered in the calculation of COP which leads to a different trend and is totally acceptable. Unlike the common closed AHTs, in which the COP is approximately 0.5, the COP values of OAHT can reach higher values, which is assumed as an advantage for OAHTs. One of the major compensations of OAHTs is their higher COPs in comparison with ordinary AHTs. As it is evident from Fig. 3, for the considered OAHT COP is more than those of common absorption heat transformers which stand

253 approximately in the range of 0.2-0.5 [29]. A similar trend has also been reported by Zhang et al [15]. This
 254 is due to the fact that the latent/sensible heat of the steam in the evaporator is recycled and then used in
 255 absorber which eradicates the demand for external heat supply. As mentioned in [12], by increasing T_{gen} ,
 256 X_s and consequently the flow ratio are boosted, which leads to the reduction of absorber heat capacity and
 257 correspondingly performance ratio which is evident on Fig. 3.

258

259 Fig. 3. Effects of T_{gen} on COP and PR of the system.

260

261 The effect of increased inlet temperature of the heat supply on the net power produced and the hydrogen
 262 production rate is displayed in Figure 4. The net power and the mass flow rate of produced hydrogen rises
 263 from 76.6 kW to 85.4 kW and 0.067 gr/s to 0.076 gr/s respectively by boosting the temperature T_7 from 100
 264 °C to 130 °C. This is due to the fact that increasing the inlet temperature of the waste heat increases the
 265 temperature of the absorber, which leads to the elevation of the evaporator's temperature [18]. Enhancing
 266 T_{eva} as the heat source of ORC-IHE boosts the net power produced by the organic Rankine cycle [21]. A
 267 portion of the turbine power is consumed for Hydrogen generation through electrolyzer. This means that by
 268 increasing the amount of power generation by turbine, the power feed to the electrolyzer will enhance which
 269 will lead to higher rate of hydrogen production [30].

270 Fig. 4. Variations of net power generation and rate of hydrogen production by waste water inlet temperature.

271 Figure 5 displays the thermal and exergy efficiencies of the integrated system as a function of waste heat
 272 inlet temperature. It is observed that as T_7 increases, both thermal and exergy efficiency increases.
 273 Referring to Figure 4, it is apparent that \dot{W}_{net} increases by boosting T_7 which has a direct impact on thermal
 274 and exergy efficiency according to equations 3 and 6. Considering the fact that the only power generation
 275 element in the integrated cycle is the turbine of ORC-IHE, it is reasonable to have an operational effect on
 276 both the efficiencies. A similar trend is reported by El-Emam and Dincer [31].

277

278

279 Fig. 5. Variations of energy and exergy efficiencies by waste water inlet temperature.

280

281 Figure 6 examines the first and second law efficiency trends against generation temperature, within a
 282 temperature range of 65- 90 °C. As is seen, both the efficiencies decrease by increasing generation
 283 temperature. This is because of the fact that while T_{gen} grows, the concentration of the strong solution will
 284 increase by enhancement of flow ratio-which will lead in lower absorption heat capacity which in turn results
 285 in lower thermal and exergy efficiency.

286 Fig. 6. Influence of T_{gen} on energy and exergy efficiencies.

287 Net power and Hydrogen productions as the functions of turbine inlet temperature have been plotted in Fig.
 288 7. It shows that net power generated increases with turbine inlet temperature. This is because of increased
 289 enthalpy at point 17 as consequence of higher turbine inlet temperature and according to equation $\dot{W}_{tur} =$
 290 $\dot{m}_{17}(h_{17} - h_{18})$, the generated power by the turbine and consequently the net power produced enhances.
 291 Increased net power output will also boost the rate of hydrogen production and once more the explanations
 292 of Figure 4 can be employed herein.

293 Fig. 7. Effect of turbine inlet temperature on net power generation and rate of hydrogen production.

294 The effect of gross temperature lift ($\Delta T = T_{abs} - T_{gen}$) on the net power produced and the rate of hydrogen
 295 production are investigated in Fig. 8. It is clear that as ΔT is increased from 0 °C to 40 °C, net power
 296 generation and rate of hydrogen production decrease by 10.8% and 12.1%. [8, 32, 33] it is clear that as
 297 T_{abs} increases, the absorber heat capacity decrease. This is due to the fact that as T_{abs} increases, X_w and
 298 consequently flow ratio (f) increase, resulting in a decrease in the absorber heat capacity. By decreasing
 299 absorber heat capacity which is considered as the heat input reduction to ORC, the net power production
 300 and correspondingly hydrogen production will decrease.

301

302 Fig. 8. Effect of gross temperature lift on net power generation and rate of hydrogen production.

303

304 The influence of entering water mass flow rate to the electrolyser on exergoenvironmental impact factor of
 305 the system is demonstrated in Fig. 9. It is revealed that by increasing the inlet water, total exergy destruction

306 of the system is decreasing which leads to the reduction of exergoenvironmental impact factor which can
307 be presumed as the better performance of the cycle. A similar trend is observed by increasing the
308 environment temperature changing from 25 °C to 35 °C.

309 Fig. 9. Effect of water mass flow rate on exergoenvironmental impact factor.

310 Fig. 10 presents the reduction of exergoenvironmental impact index by the growth of evaporator
311 temperature. The reason is that, by boosting evaporator temperature, exergetic efficiency and internal
312 exergy rate increase which causes a slight decline in the exergoenvironmental impact index. Once more
313 by increasing environmental temperature, exergoenvironmental impact index decreases. By recalling the
314 fact that the desired condition is the minimum quantity of exergoenvironmental impact index, both the latter
315 mentioned variations, are beneficial.

316 Fig. 10. Effect of evaporator temperature on the exergoenvironmental impact index.

317 The effect of evaporator temperature on the exergoenvironmental impact improvement has been plotted
318 on Fig. 11. It is obvious that by raising the evaporator temperature, the exergoenvironmental impact index
319 of the system is increasing. As mentioned earlier, the higher amount of exergoenvironmental impact index,
320 the better environmental influence. Thus, from this point of view, increasing evaporator temperature has an
321 advantageous trend. The same tendency is observed while environment temperature is boosted.

322 Fig. 11. Effect of evaporator temperature on the exergoenvironmental impact improvement.

323 The effect of evaporator temperature on the exergetic stability factor, has been plotted on Fig. 12. According
324 to the definition of exergetic stability factor, the optimum operation is while its quantity is close to one which
325 is completely acceptable according to its definition. As is obvious from Fig.12, there is an increasing
326 approaching trend to “one” for the exergetic stability factor by increasing the evaporator temperature. This
327 clarifies the fact that by increasing evaporator temperature, less exergy destruction rate is achieved. It
328 would be noted that herein, no fuel is consumed. The trend of environment temperature is similar to
329 exergoenvironmental impact index demonstrated in previous diagram.

330 Figure. 12. Effect of evaporator temperature on the exergetic stability factor.

331 Fig. 13 illustrates the relation between evaporator temperature and exergetic sustainability index. By the

332 growth of evaporator temperature from 115 °C to 120 °C, exergetic sustainability index is increasing which
333 is considered as an advantage for the system. Once more by enhancing environment temperature, cycle
334 performs better and higher amount of exergetic sustainability index is attained.

335 Figure. 13. Effect of evaporator temperature on the exergetic sustainability index.

336 V. Conclusion

337

338 An analysis of a novel multi-generation system including an open absorption heat transformer (OAHT), an
339 organic Rankine cycle with Internal Heat Exchanger and an electrolyzer was studied. Based on energy,
340 exergy and exergoenvironmental analyses through the code developed in Engineering Equation Solver and
341 results presented in the paper, following conclusions are made:

- 342 ➤ By increasing T_{gen} , COP of the OAHT decreases, which is in contradiction to the results obtained
343 in ordinary AHTs incorporated with a desalination system.
- 344 ➤ The net power output and the hydrogen production rate increase by boosting the inlet temperature
345 of the waste heat.
- 346 ➤ Both thermal and exergy efficiency of the integrated system will increase when the inlet temperature
347 of the waste heat increases.
- 348 ➤ Generation temperature has an opposite impact on the thermal and exergy efficiency.
- 349 ➤ Increasing the inlet water mass flow rate to the electrolyzer, the exergoenvironmental impact factor
350 reduces which can be presumed as the better performance of the cycle.
- 351 ➤ By the growth of evaporator temperature, exergoenvironmental impact index, exergoenvironmental
352 impact index, exergetic stability factor and exergetic sustainability index is increasing which is
353 advantageous for the environment.

354 VI. Future work

355

356 Considering the importance of exergoeconomic analysis, as the second stage of the current work, authors
357 will investigate the exergoeconomic model of the current research in terms of cost-optimal design point of
358 view.

359

360

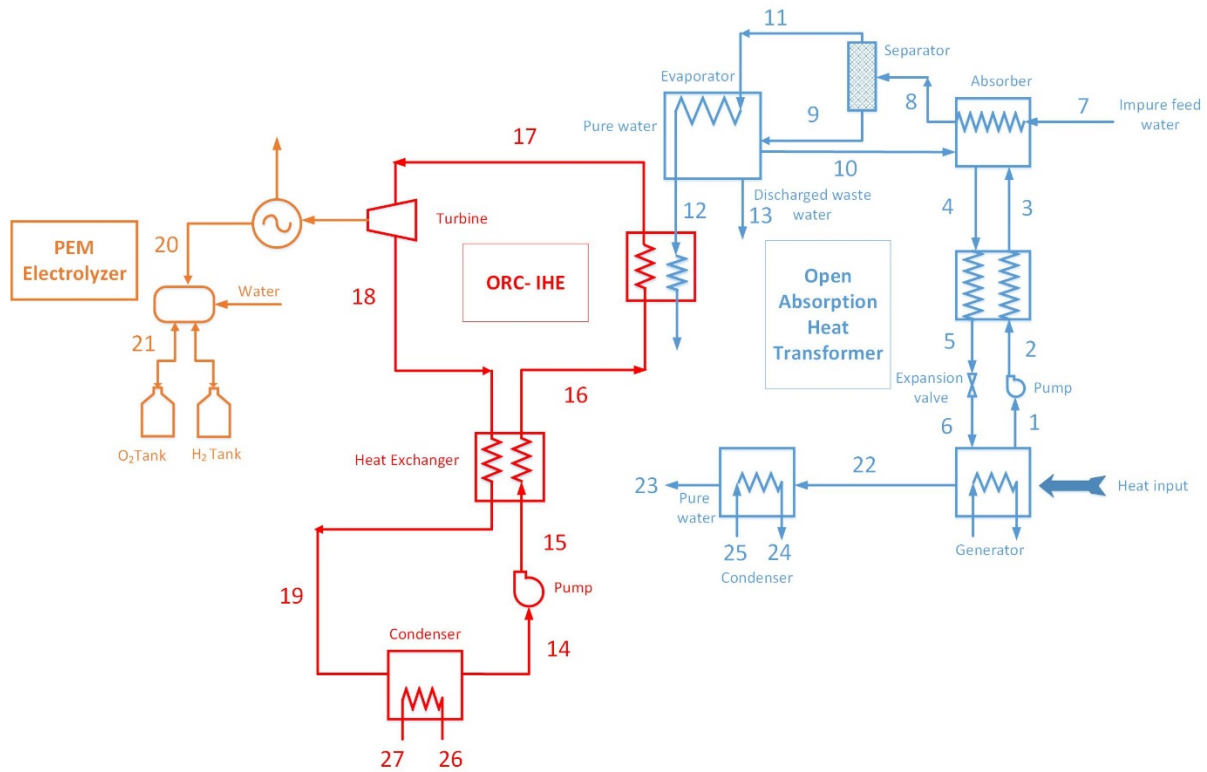
References

- 361
362
363
364 [1] Ma Z, Bao H, Roskilly AP. Performance analysis of ultralow grade waste heat upgrade using absorption heat
365 transformer. *Applied Thermal Engineering*.
366 [2] Vélez F, Segovia JJ, Martín MC, Antolín G, Chejne F, Quijano A. A technical, economical and market review of
367 organic Rankine cycles for the conversion of low-grade heat for power generation. *Renewable and Sustainable Energy*
368 *Reviews*. 2012;16(6):4175-89.
369 [3] Zhang X, He M, Zhang Y. A review of research on the Kalina cycle. *Renewable and Sustainable Energy Reviews*.
370 2012;16(7):5309-18.
371 [4] Zhai XQ, Qu M, Li Y, Wang RZ. A review for research and new design options of solar absorption cooling
372 systems. *Renewable and Sustainable Energy Reviews*. 2011;15(9):4416-23.
373 [5] Li T, Yu H, Li Y-Y, Liu Q, Chen C, Guo L, et al. Study on washwater effluent quality discharged by ship exhaust
374 gas DeSO_x system with magnesium and seawater desulphurisation method. *International Journal of Environment and*
375 *Pollution*. 2014;56(1-4):1-10.
376 [6] Khamooshi M, Parham K, Atikol U. Overview of ionic liquids used as working fluids in absorption cycles.
377 *Advances in Mechanical Engineering*. 2013;2013.
378 [7] Fang H, Xia J, Zhu K, Su Y, Jiang Y. Industrial waste heat utilization for low temperature district heating. *Energy*
379 *policy*. 2013;62:236-46.
380 [8] Parham K, Yari M, Atikol U. Alternative absorption heat transformer configurations integrated with water
381 desalination system. *Desalination*. 2013;328:74-82.
382 [9] Parham K, Khamooshi M, Tematio DBK, Yari M, Atikol U. Absorption heat transformers - A comprehensive
383 review. *Renewable and Sustainable Energy Reviews*. 2014;34:430-52.
384 [10] Donnellan P, Cronin K, Byrne E. Recycling waste heat energy using vapour absorption heat transformers: A
385 review. *Renewable and Sustainable Energy Reviews*. 2015;42:1290-304.
386 [11] Khamooshi M, Parham K, Egelioglu F, Yari M, Salati H. Simulation and optimization of novel configurations of
387 triple absorption heat transformers integrated to a water desalination system. *Desalination*. 2014;348:39-48.
388 [12] Khamooshi M, Parham K, Roozbeh I, Ensafisoroor H. Applications of innovative configurations of double
389 absorption heat transformers in water purification technology. *Desalination and Water Treatment*. 2016;57(18):8204-
390 16.
391 [13] Parham K, Atikol U, Yari M, Agboola OP. Evaluation and optimization of single stage absorption chiller using
392 (LiCl + H₂O) as the working pair. *Advances in Mechanical Engineering*. 2013;2013.
393 [14] Rivera W, Romero R, Cardoso M, Aguillón J, Best R. Theoretical and experimental comparison of the
394 performance of a single - stage heat transformer operating with water/lithium bromide and water/Carrol™.
395 *International journal of energy research*. 2002;26(8):747-62.
396 [15] Horuz I, Kurt B. Absorption heat transformers and an industrial application. *Renewable Energy*.
397 2010;35(10):2175-81.
398 [16] Ensafisoroor H, Khamooshi M, Egelioglu F, Parham K. An experimental comparative study on different
399 configurations of basin solar still. *Desalination and Water Treatment*. 2016;57(5):1901-16.
400 [17] Zhang X, Hu D, Li Z. Performance analysis on a new multi-effect distillation combined with an open absorption
401 heat transformer driven by waste heat. *Applied Thermal Engineering*. 2014;62(1):239-44.
402 [18] Hamidi A, Parham K, Atikol U, Shahbaz AH. A parametric performance analysis of single and multi-effect
403 distillation systems integrated with open-cycle absorption heat transformers. *Desalination*. 2015;371:37-45.
404 [19] Khamooshi M, Parham K, Yari M, Egelioglu F, Salati H, Babadi S. Thermodynamic analysis and optimization
405 of a high temperature triple absorption heat transformer. *Scientific World Journal*. 2014;2014.
406 [20] Quoilin S, Van Den Broek M, Declaye S, Dewallef P, Lemort V. Techno-economic survey of Organic Rankine
407 Cycle (ORC) systems. *Renewable and Sustainable Energy Reviews*. 2013;22:168-86.
408 [21] Zare V. A comparative exergoeconomic analysis of different ORC configurations for binary geothermal power
409 plants. *Energy Conversion and Management*. 2015;105:127-38.
410 [22] Hamada Y, Takeda K, Goto R, Kubota H. Hybrid utilization of renewable energy and fuel cells for residential
411 energy systems. *Energy and Buildings*. 2011;43(12):3680-4.
412 [23] Asghari S, Mokmeli A, Samavati M. Study of PEM fuel cell performance by electrochemical impedance
413 spectroscopy. *International Journal of Hydrogen Energy*. 2010;35(17):9283-90.
414 [24] Midilli A, Dincer I. Development of some exergetic parameters for PEM fuel cells for measuring environmental
415 impact and sustainability. *International Journal of Hydrogen Energy*. 2009;34(9):3858-72.
416 [25] Klein SA, F A. *Engineering Equation Solver, F-Chart Software*. Middelton. 2012.

- 417 [26] Ratlamwala TAH, Dincer I, Reddy BV. Exergetic and environmental impact assessment of an integrated system
418 for utilization of excess power from thermal power plant. *Causes, Impacts and Solutions to Global Warming* 2013. p.
419 803-24.
- 420 [27] Ratlamwala TAH, Dincer I, Gadalla MA. Comparative environmental impact and sustainability assessments of
421 hydrogen and cooling production systems. *Causes, Impacts and Solutions to Global Warming* 2013. p. 389-408.
- 422 [28] Rivera W, Cerezo J, Rivero R, Cervantes J, Best R. Single stage and double absorption heat transformers used to
423 recover energy in a distillation column of butane and pentane. *International Journal of Energy Research*.
424 2003;27(14):1279-92.
- 425 [29] Parham K, Khamooshi M, Daneshvar S, Assadi M, Yari M. Comparative assessment of different categories of
426 absorption heat transformers in water desalination process. *Desalination*. 2016;396:17-29.
- 427 [30] Ratlamwala TAH, Dincer I. Development of a geothermal based integrated system for building multigenerational
428 needs. *Energy and Buildings*. 2013;62:496-506.
- 429 [31] El-Emam RS, Dincer I. Exergy and exergoeconomic analyses and optimization of geothermal organic Rankine
430 cycle. *Applied Thermal Engineering*. 2013;59(1):435-44.
- 431 [32] Gomri R. Thermal seawater desalination: Possibilities of using single effect and double effect absorption heat
432 transformer systems. *Desalination*. 2010;253(1-3):112-8.
- 433 [33] Romero RJ, Rodríguez-Martínez A. Optimal water purification using low grade waste heat in an absorption heat
434 transformer. *Desalination*. 2008;220(1):506-13.
- 435
436
437
438
439
440
441
442
443
444
445
446
447
448
449
450
451
452
453
454
455
456
457
458
459
460
461
462
463
464
465
466
467
468
469
470
471
472

473 *Figures:*

474

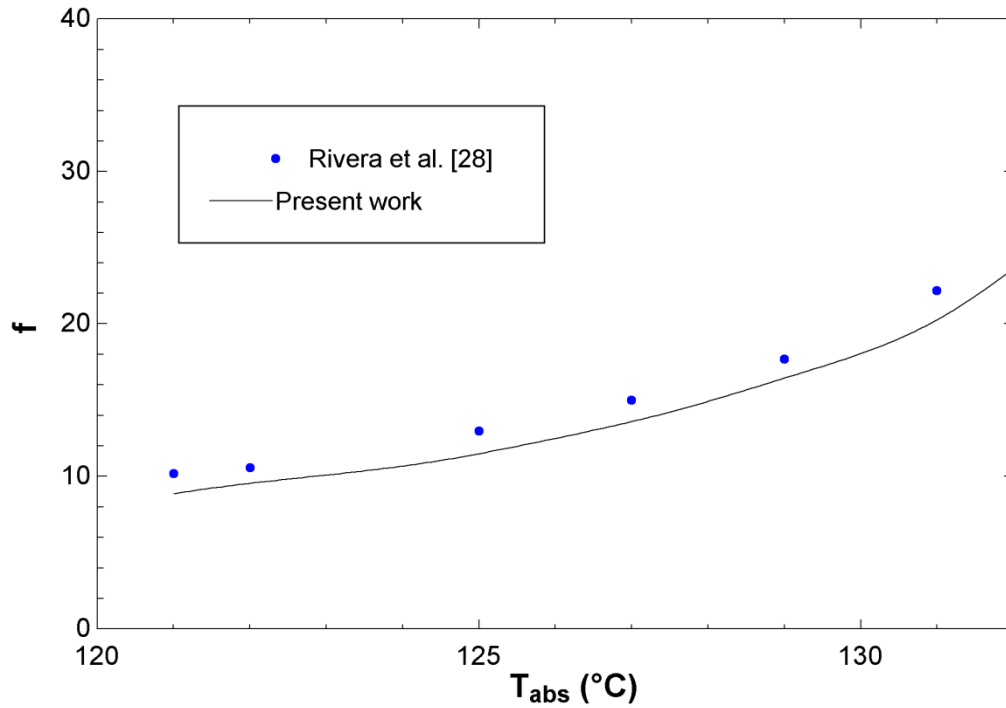


475

476

477

Fig. 1. Schematic illustration of the proposed cycle.

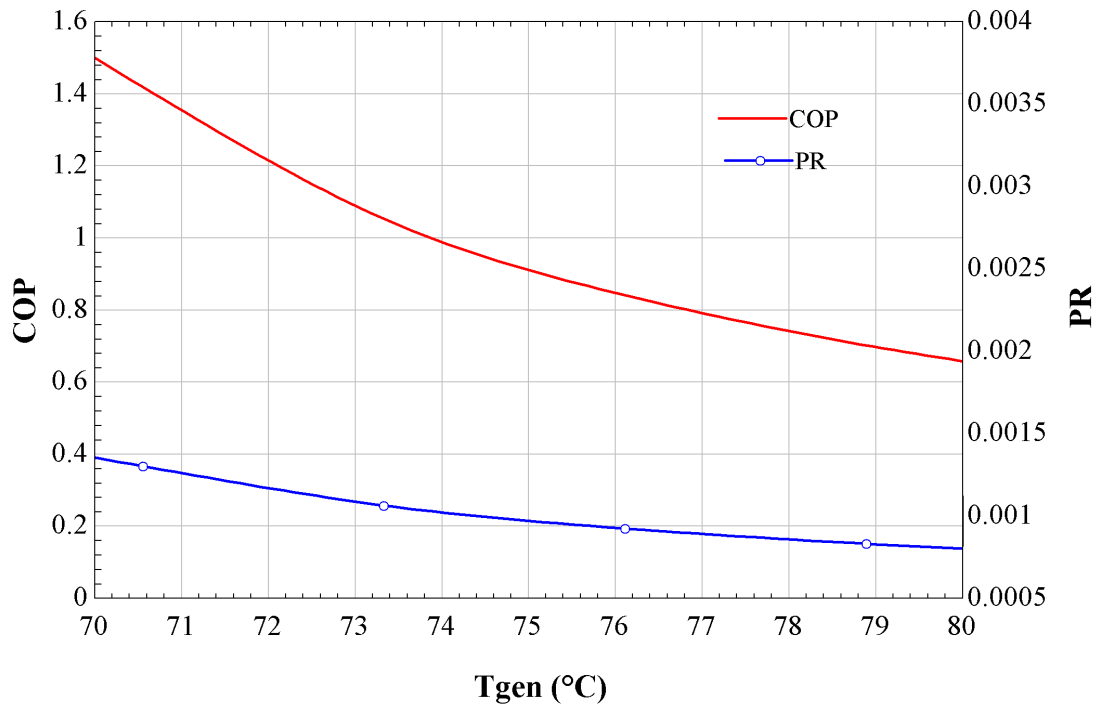


478

479

480

Fig. 2. Comparison of the simulation results with those of Rivera et al [28].

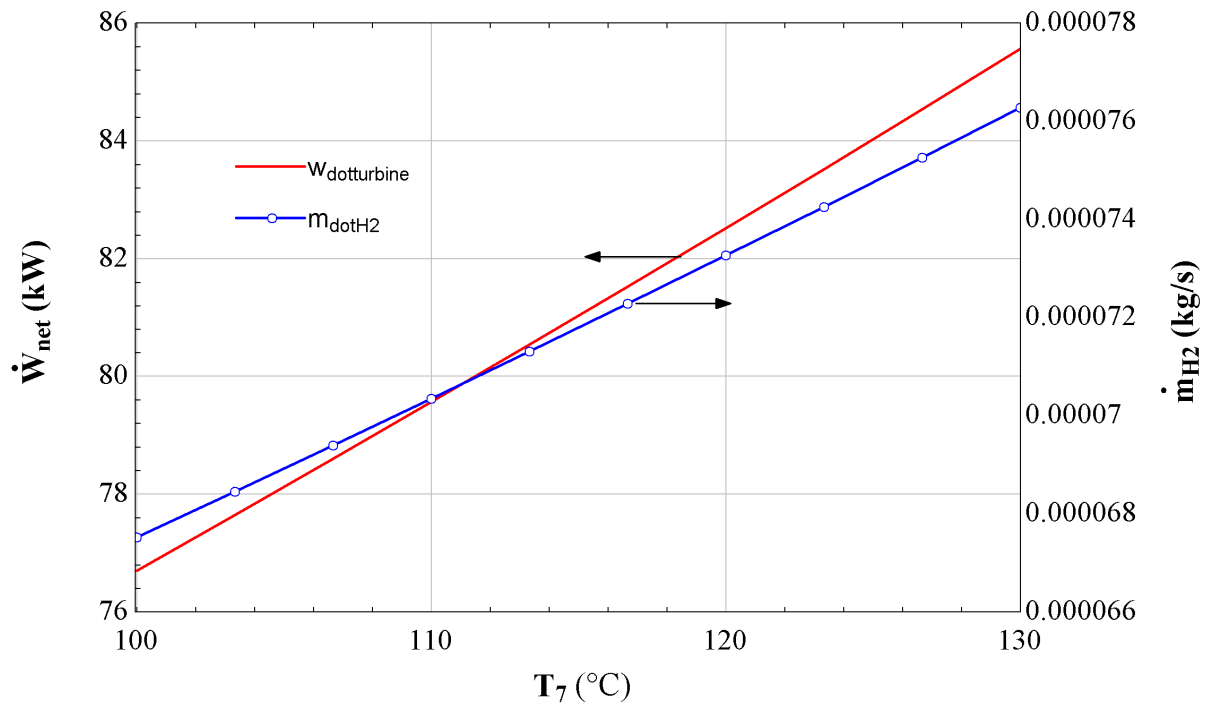


481

482

Fig. 3. Effects of T_{gen} on COP and PR of the system.

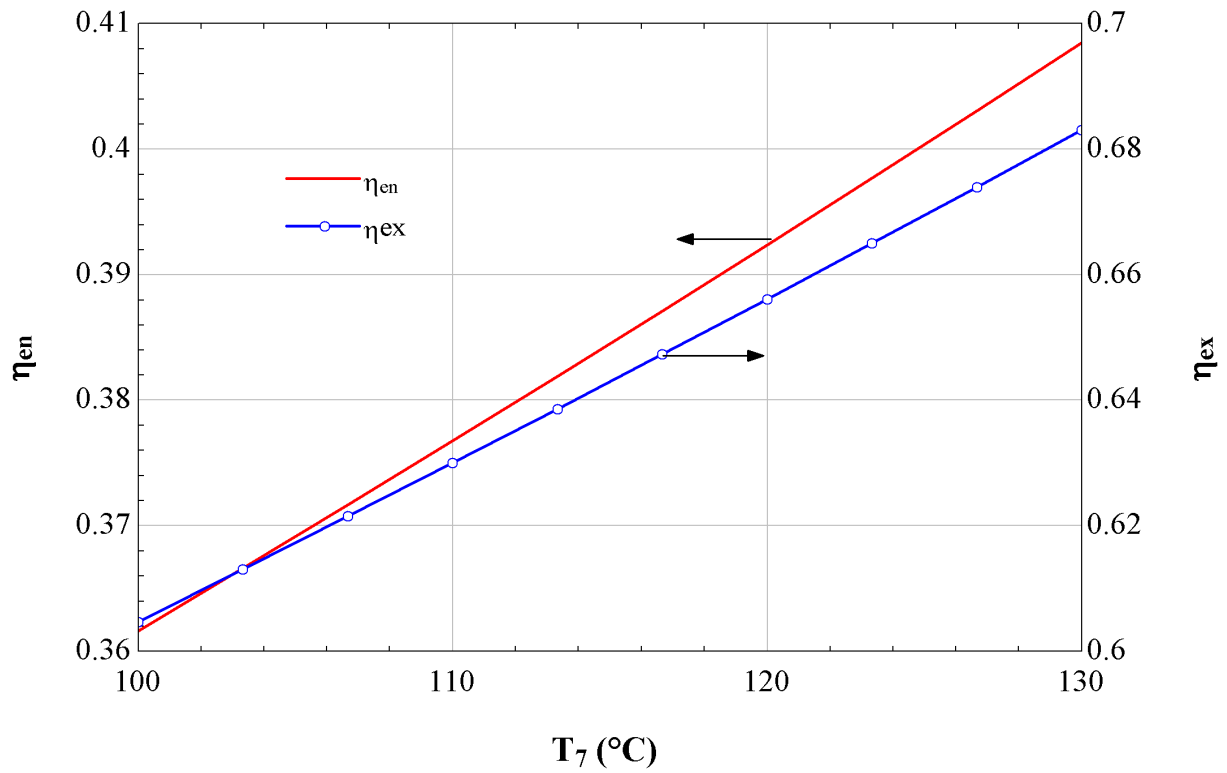
483



484

485

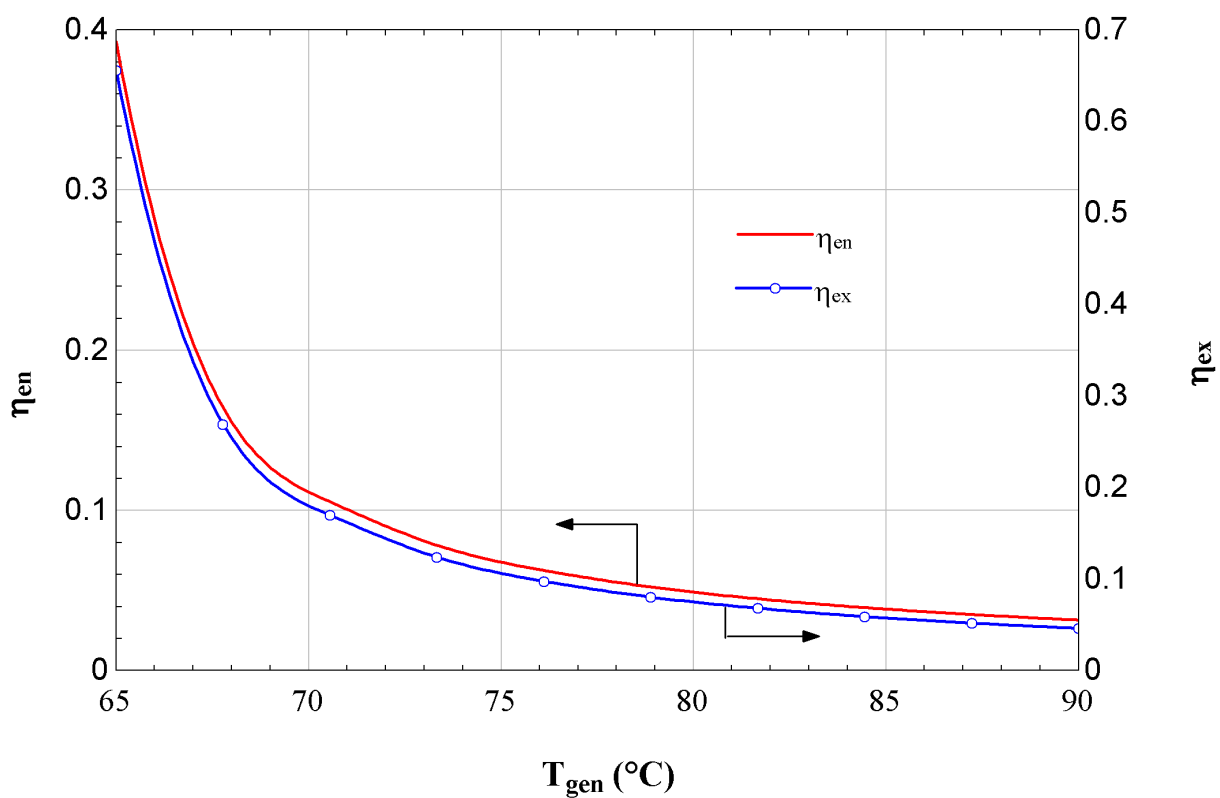
Fig. 4. Variations of net power generation and rate of hydrogen production by wastewater inlet temperature.



486

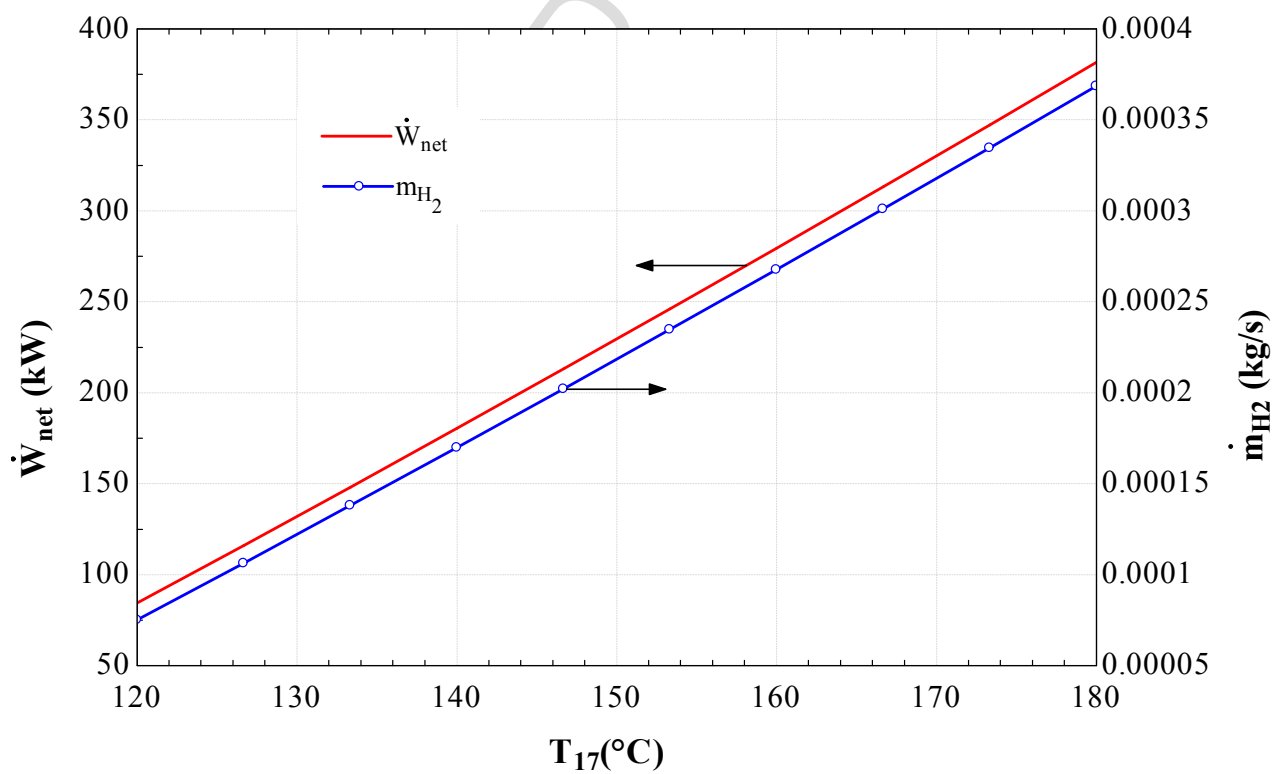
487

Fig. 5. Variations of energy and exergy efficiencies by waste water inlet temperature.



488

489

Fig. 6. Influence of T_{gen} on energy and exergy efficiencies.

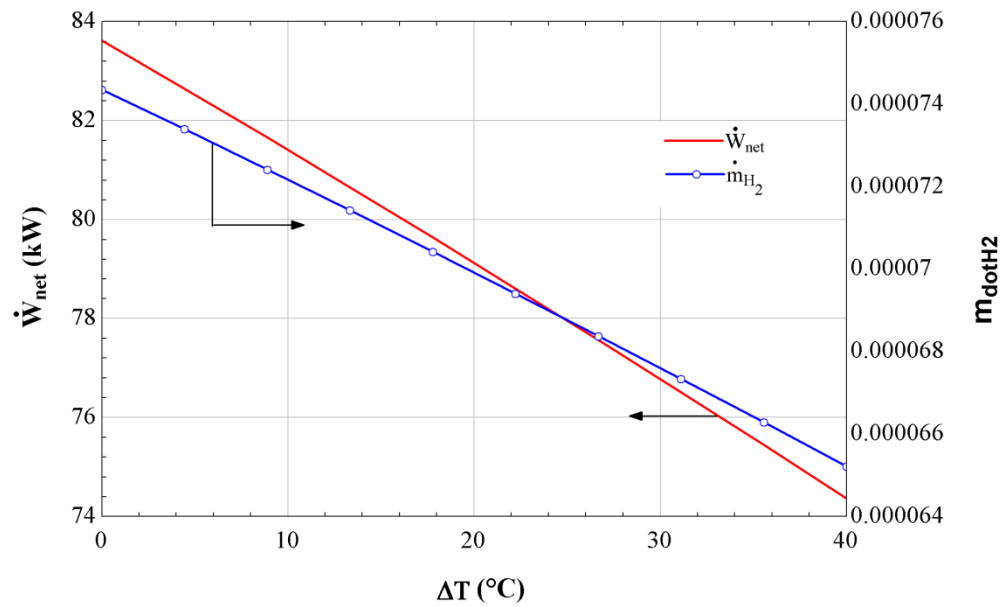
490

491

492

Fig. 7. Effect of turbine inlet temperature on net power generation and rate of hydrogen production.

493



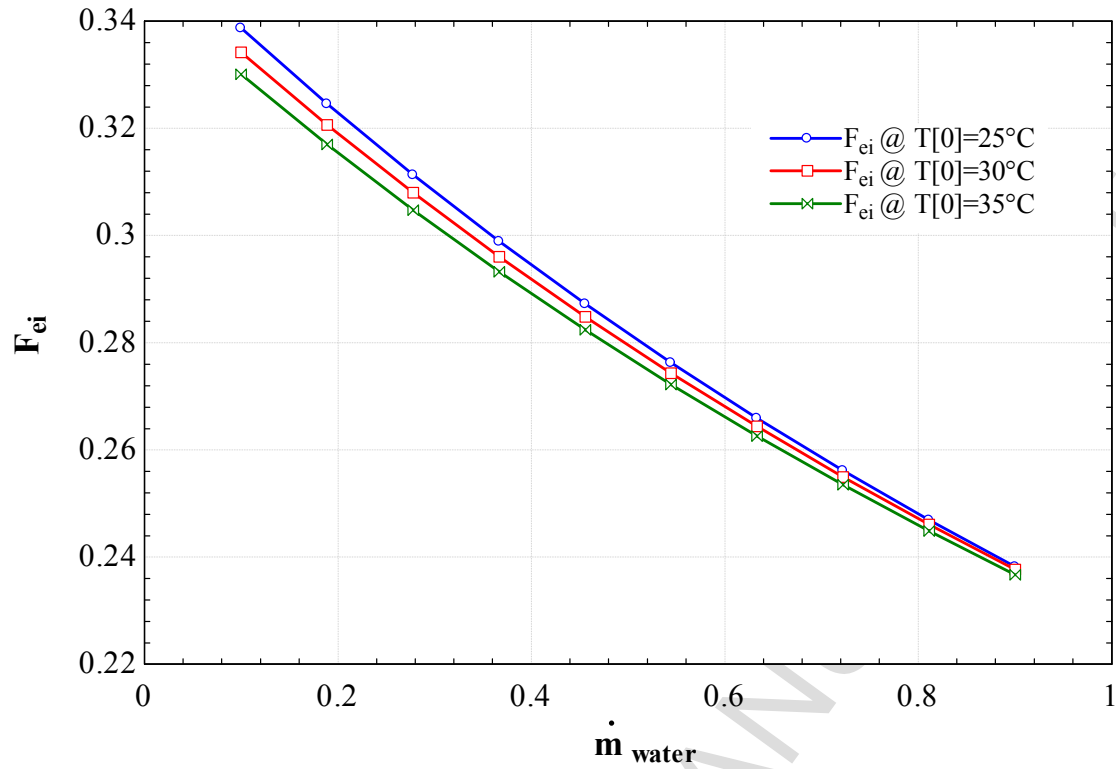
494

495

Fig. 8. Effect of gross temperature lift on net power generation and rate of hydrogen production.

496

497

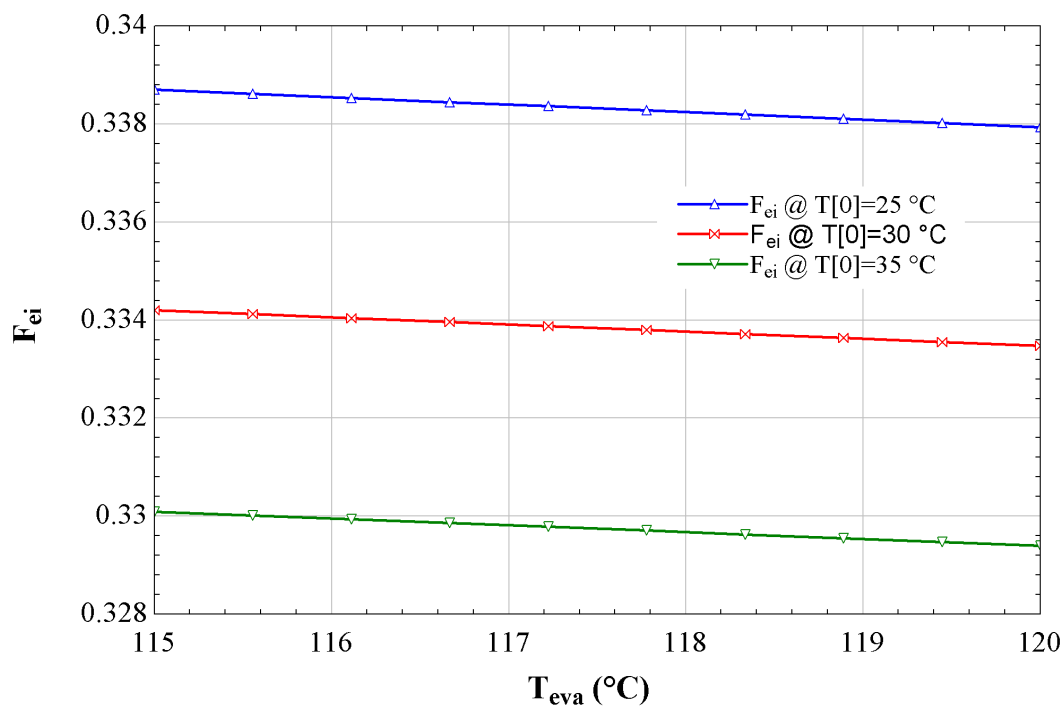


498

499

500

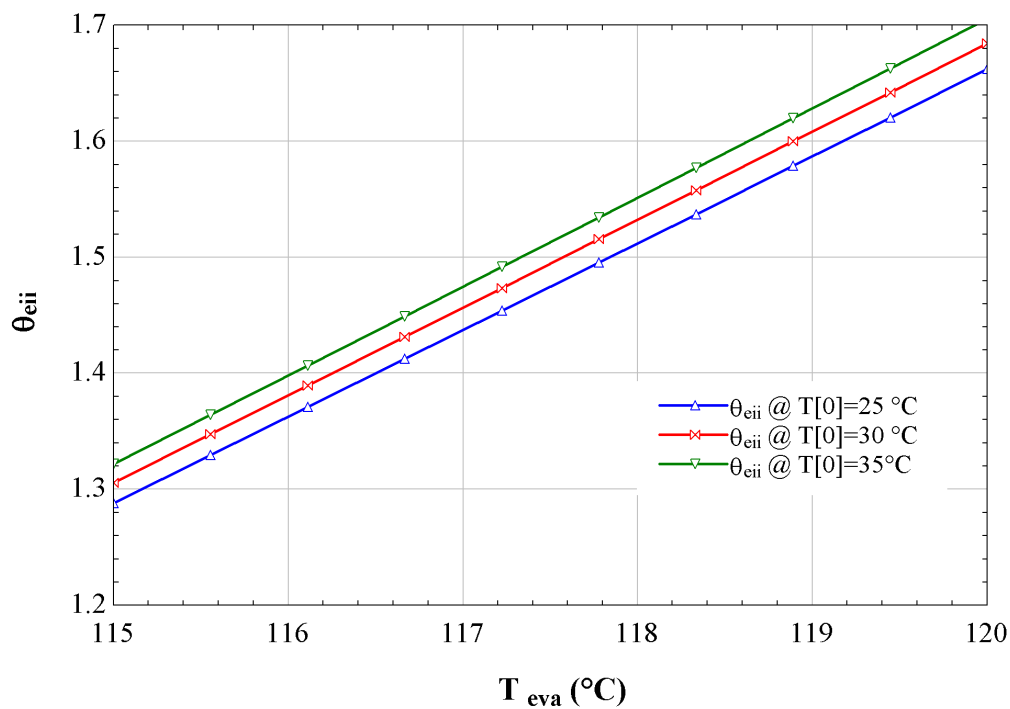
Fig. 9. Effect of water mass flow rate on exergoenvironmental impact factor.



501

502

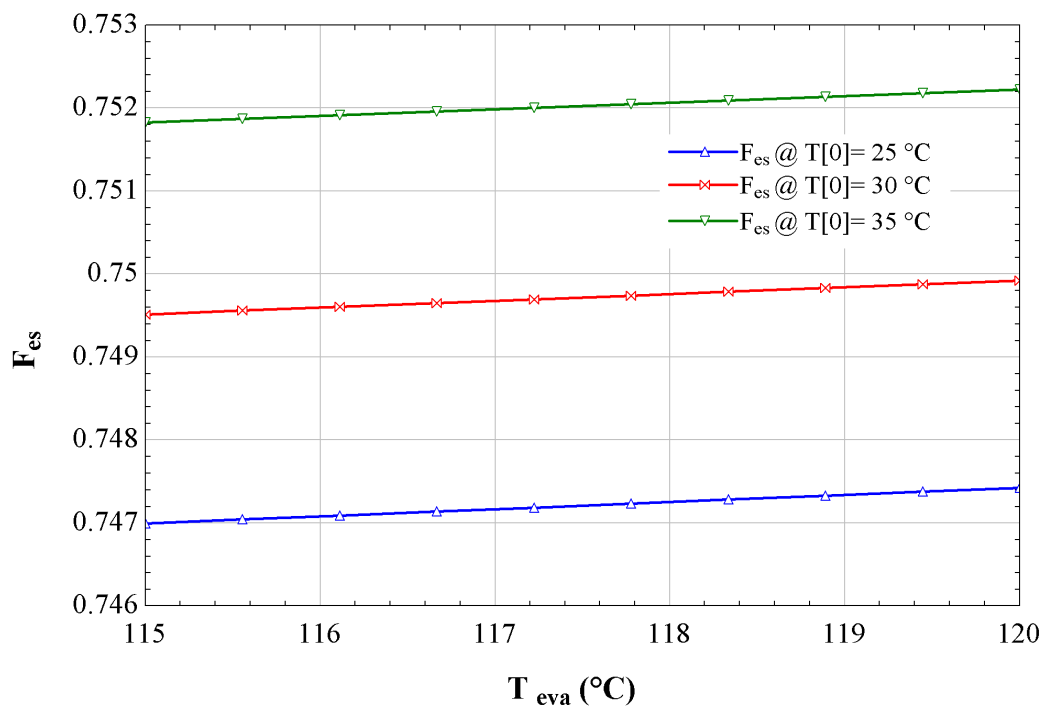
Fig. 10. Effect of evaporator temperature on the exergoenvironmental impact index.



503

504

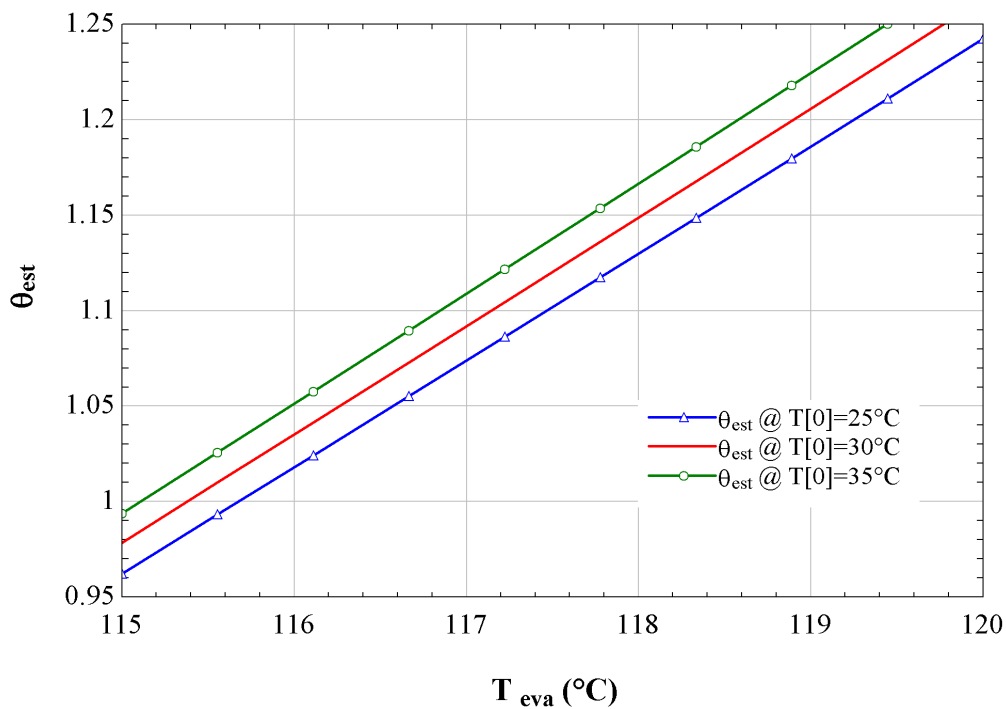
Fig. 21. Effect of evaporator temperature on the exergoenvironmental impact improvement.



505

506

Figure. 12. Effect of evaporator temperature on the exergetic stability factor.



507

508

Figure. 13. Effect of evaporator temperature on the exergetic sustainability index.

509 *Tables:*
 510
 511

| | |
|---------------------------------|--|
| $T_0 = 30$ (°C) | Ambient Temperature |
| $\omega = 40\%$ | Specific Humidity of the Ambient Air |
| $P_0 = 101$ (kPa) | Ambient Pressure |
| $\eta_{elec} = 56\%$ | Electrolyzer Efficiency |
| $T_{water,in} = 25$ (°C) | Temperature of the Water Injected to Electrolyzer |
| $\dot{m}_{water,in} = 1$ (kg/s) | Mass Flow Rate of the Water Injected to Electrolyzer |

512
 513
 514
 515

Table. 1. The Initial Design and Operation Parameters of the System.

| State Points | Temperature (°C) | Specific enthalpy (kJ/kg) | Pressure (kPa) | Mass flow rate (kg/s) | Specific entropy (kJ/kg K) |
|--------------|------------------|---------------------------|----------------|-----------------------|----------------------------|
| 0 | 35 | 129.4 | 101 | - | 5.764 |
| 1 | 65 | 138.2 | 7.381 | 3 | 0.4522 |
| 2 | 65 | 138.2 | 198.5 | 3 | 0.4522 |
| 3 | 98 | 212.4 | 198.5 | 3 | 0.6604 |
| 4 | 125 | 281.6 | 101 | 3.265 | 0.8834 |
| 5 | 125 | 281.6 | 101 | 3.265 | 0.8834 |
| 6 | 56.57 | 281.6 | 7.381 | 3.265 | 0.4398 |
| 7 | 120 | 503.8 | 198.5 | 0.1 | 1.528 |
| 8 | 120 | 1504 | 101.5 | 0.1 | 7.459 |
| 9 | 120 | 503.8 | 198.5 | 0.05459 | 1.528 |
| 10 | 120 | 2706 | 198.5 | 0.04959 | 7.13 |
| 11 | 120 | 2706 | 198.5 | 0.04541 | 7.13 |
| 12 | 120 | 503.8 | 198.5 | 0.04541 | 1.528 |
| 13 | 120 | 503.8 | 198.5 | 0.005 | 1.528 |

| | | | | | |
|----|-------|-------|-------|----------------|--------|
| 14 | 85 | 542.3 | 250 | 2 | 1.827 |
| 15 | 85 | 538.1 | 400 | 2 | 1.749 |
| 16 | 120 | 606.6 | 400 | 2 | 1.931 |
| 17 | 124.6 | 615.9 | 400 | 2 | 1.954 |
| 18 | 100 | 570.7 | 250 | 2 | 1.904 |
| 19 | 70 | 514.6 | 250 | 2 | 1.748 |
| 20 | - | - | - | - | - |
| 21 | 25 | 0 | 101 | \dot{M}_{H2} | 64.78 |
| 22 | 65 | 2621 | 7.381 | 0.2648 | 8.401 |
| 23 | 40 | 167.5 | 7.381 | 0.2648 | 0.5723 |

516

517

Table. 2. Thermodynamic properties of the System at each state point.

518

519

1. A novel cycle has been proposed for producing water, power and Hydrogen.
2. To assess the cycle's performance a model has been developed in EES.
3. First and second laws of thermodynamics besides exergoenvironmental analysis have been investigated.
4. Imperative system parameters are studied.